Troposelective Substitutions in Microsolvated Systems

A. Filippi and M. Speranza*

Contribution from the Dipartimento di Studi di Chimica e Tecnologia delle Sostanze Biologicamente Attive, Università degli Studi di Roma "La Sapienza", P.le A. Moro 5, I-00185 Roma, Italy

Received December 15, 2000

Abstract: The mechanism and the stereochemistry of the intracomplex "solvolysis" of the proton-bound complexes $\mathbf{I^X}$ between $CH_3{}^{18}OH$ and (*R*)-(+)-1-aryl-ethanol ($\mathbf{1_R{}^X}$; aryl = phenyl (X = H); pentafluorophenyl (X = F)) have been investigated in the gas phase in the 25−100 °C temperature range. The results point to intracomplex "solvolysis" as proceeding through the intermediacy of the relevant benzyl cation $\mathbf{III^X}$ (a pure S_N1 mechanism). "Solvolysis" of $\mathbf{I^H}$ leads to complete racemization at $T > 50$ °C, whereas at $T < 50$ °C the reaction displays a preferential retention of configuration. Predominant retention of configuration is also observed in the intracomplex "solvolysis" of $\mathbf{I^F}$. This picture is rationalized in terms of different intracomplex interactions between the benzylic ion $\mathbf{III^X}$ and the nucleophile/leaving group pair, which govern the timing of their reorientation within the electrostatic complex. The obtained gas-phase picture is discussed in the light of related gas-phase and solution data. It is concluded that the solvolytic reactions are mostly governed by the lifetime and the dynamics of the species involved and, if occurring in solution, by the nature of the solvent cage. Their rigid subdivision into the S_N1 and S_N2 mechanistic categories appears inadequate, and the use of their stereochemistry as a mechanistic probe can be highly misleading.

Introduction

The concept of solvolytic reactions involving the intermediacy of a free carbocation (S_N1)[1] has been repeatedly modified and refined in the past 60 years.[2] This continuous adjustment is a symptom of the difficulty of proving the unimolecularity of a solvolytic reaction by kinetics when the nucleophile is the solvent. Assessment of the mechanism of a solvolytic process is based essentially on the stereochemical distribution of the products. In general, a bimolecular S_N2 reaction involves predominant inversion of configuration of the reaction center. A unimolecular S_N1 displacement instead proceeds through the intermediacy of a free carbocation and, therefore, usually leads to a racemate. However, many alleged S_N1 solvolyses do not give fully racemized products. The enantiomer in excess often, but not always, corresponds to inversion. Furthermore, the stereochemical distribution of products may be highly sensitive to the solvolytic conditions.[3] These observations have led to the concept of competing[4−6] or mixed[6,7] S_N1-S_N2 mechanisms. More recently, the existence of S_N1 reactions in itself has been put into question.[8]

The aim of this work is to uncover the stereochemistry and the intimate mechanism of a model "solvolytic" reaction taking place in a ion−dipole pair in the gaseous phase. An isolated ion−dipole complex is a microscopic system held together by attractive electrostatic interactions. It represents a model for analogous intimate ion−molecule pairs restrained in the solvent cage in solution.[9] The main difference is that the behavior of an isolated ion−dipole complex is not perturbed by those environmental factors (solvation, ion pairing, etc.) which normally affect the fate of intimate ion−dipole pairs in solution. Hence, a detailed study of the "solvolysis" of an isolated proton-bound complex, such as $\mathbf{I^X}$ of Scheme 1, may provide valuable information on the intrinsic factors governing the reaction and how these factors may be influenced by the solvent cage in solution.

Adduct $\mathbf{I^X}$ is obtained in the gas phase by association of the relevant chiral alcohol $\mathbf{1_R{}^X}$ with the $CH_3{}^{18}OH_2{}^+$ ion, generated by γ-radiolysis of $CH_3F/H_2{}^{18}O$ mixtures (Scheme 2; Y = F).[10] This approach allows formation of $\mathbf{I^X}$ in a gaseous inert medium (CH_3F) at pressures high enough (720 Torr) to ensure its complete thermalization. Furthermore, generation of the complex $\mathbf{I^X}$ takes place in the absence of neutral "solvent" molecules, i.e., $CH_3{}^{18}OH$. Hence, the formation of ^{18}O-labeled[11] ethers $\mathbf{2_R{}^X}$ and $\mathbf{2_S{}^X}$ of Scheme 1 must be necessarily traced to the *intracomplex* "solvolysis" of $\mathbf{I^X}$.

Ancillary experiments have been carried out to evaluate the extent of $\mathbf{II_R{}^X \rightleftarrows II_S{}^X}$ interconversion (k_{inv} in Scheme 1) prior to

(1) Hughes, E. D.; Ingold, C. K. *J. Chem. Soc.* **1935**, 244.
(2) Winstein, S.; Clippinger, E.; Feinberg, A. H.; Heck, R.; Robinson, G. C. *J. Am. Chem. Soc.* **1956**, *78*, 328.
(3) March, J. *Advanced Organic Chemistry*; Wiley: New York, 1985.
(4) Dostrovsky, I.; Hughes, E. D.; Ingold, C. K. *J. Chem. Soc.* **1946**, 173.
(5) Bentley, T. W.; Bowen, C. T.; Parker, W.; Watt, C. I. F. *J. Am. Chem. Soc.* **1979**, *101*, 2486.
(6) Jencks, W. P. *Chem. Soc. Rev.* **1982**, *10*, 345.
(7) (a) Bentley, T. W.; Bowen, C. T.; Morten, D. H.; Schleyer, P. v. R. *J. Am. Chem. Soc.* **1981**, *103*, 5466. (b) Bentley, T. W.; Bowen, C. T. *J. Chem. Soc., Perkin Trans. 2* **1978**, 557.
(8) Dale, J. *J. Chem. Educ.* **1998**, *75*, 1482.
(9) (a) McAdoo, D. J.; Morton, T. H. *Acc. Chem. Res.* **1993**, *26*, 295. (b) Morton, T. H. *Org. Mass Spectrom.* **1992**, *27*, 353. (c) Morton, T. H. *Tetrahedron* **1982**, *38*, 3195.
(10) Each elementary step of Scheme 2 is highly efficient (Blint, R. J.; McMahon, T. B.; Beauchamp, J. L. *J. Am. Chem. Soc.* **1974**, *96*, 1269. Troiani, A.; Filippi, A.; Speranza, M. *Chem. Eur. J.* **1997**, *3*, 2063).
(11) $H_2{}^{16}O$ is a ubiquitous impurity present in the gaseous systems, either initially introduced with their bulk component or formed from their radiolysis. As pointed out previously (Troiani, A.; Gasparrini, F.; Grandinetti, F.; Speranza, M. *J. Am. Chem. Soc.* **1997**, *119*, 4525), the average stationary concentration of $H_2{}^{16}O$ in the irradiated systems is estimated to approach that of the added $H_2{}^{18}O$ (ca. 2−3 Torr). Apart from $CH_3{}^{16}OH_2{}^+$, deriving from $(CH_3)_2F^+$ attack on ubiquitous water (Scheme 2; Y = F), unlabeled ethers may arise from direct attack of the $(CH_3)_2F^+$ ions on $\mathbf{1_R{}^X}$.

10.1021/ja004265p CCC: $20.00
Published on Web 06/02/2001

Scheme 1

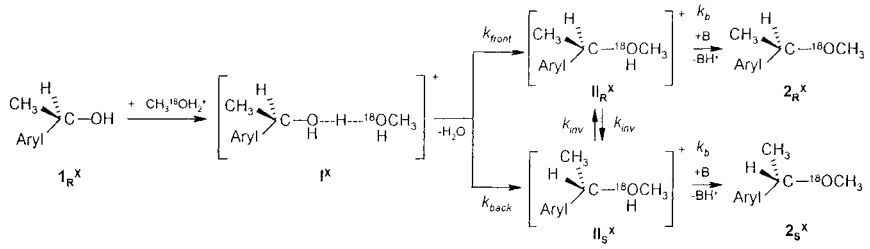

Scheme 2

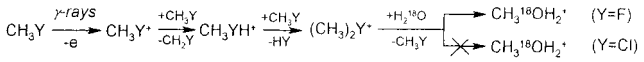

neutralization (k_b in Scheme 1). The gaseous samples used to this purpose contained CH_3Cl, instead of CH_3F, as the bulk component. This prevents the radiolytic formation of $CH_3{}^{18}OH_2^+$ ions to any significant extent. In fact, unlike $(CH_3)_2F^+$, $(CH_3)_2Cl^+$ ions are essentially inert toward the water molecules present in the mixture (Scheme 2; Y = Cl).[12] As a consequence, the oxonium intermediates $\mathbf{II_R^X}$ are directly formed from $(CH_3)_2Cl^+$ methylation of $\mathbf{1_R^X}$, and any contribution from other conceivable pathways, including the second step of Scheme 1, can be safely excluded.[13]

Experimental Section

Materials. Methyl fluoride, methyl chloride, and oxygen were high-purity gases from UCAR Specialty Gases N.V., used without further purification. Samples of $H_2{}^{18}O$ (^{18}O content > 97%) and $(C_2H_5)_3N$ were purchased from ICON Services and Aldrich Co., respectively. (*R*)-(+)-1-Phenylethanol ($\mathbf{1_R^H}$) and its *S*-enantiomer ($\mathbf{1_S^H}$) and (*R*)-(+)-1-pentafluorophenylethanol ($\mathbf{1_R^F}$) and its *S*-enantiomer ($\mathbf{1_S^F}$) were research grade chemicals from Aldrich Co. Alcohols $\mathbf{1_R^H}$ and $\mathbf{1_R^F}$, used as starting substrates, were purified by enantioselective semipreparative HPLC on a chiral column, (*R*,*R*)-Ulmo, 5 μm, 250 × 4.6 mm i.d., eluent 99/1 (v/v) *n*-hexane/propan-2-ol, flow rate 1.0 mL·min^{-1}, detection by UV (254 nm) and ORD (polarimeter) in series; and by enantioselective HRGC [(i) MEGADEX DACTBS-β (30% 2,3-di-*O*-acetyl-6-*O*-*tert*-butyldimethylsilyl-β-cyclodextrin in OV 1701; 25 m long, 0.25 mm i.d, d_f = 0.25 μm) fused silica column, at 60 < *T* <170 °C, 4 °C min^{-1}; (ii) MEGADEX 5 (30% 2,3-di-*O*-methyl-6-*O*-pentyl-β-cyclodextrin in OV 1701; 25 m long, 0.25 mm i.d, d_f = 0.25 μm) fused silica column at *T* = 125 °C. (*S*)-(−)-1-Phenyl-1-methoxyethane ($\mathbf{2_S^H}$) and its *R*-enantiomer ($\mathbf{2_R^H}$) and (*S*)-(−)-1-pentafluorophenyl-1-methoxyethane ($\mathbf{2_S^F}$) and its *R*-enantiomer ($\mathbf{2_R^F}$) were synthesized from the corresponding alcohols by the dimethyl sulfate method.[14] Their identities were verified by spectroscopic methods.

Procedure. The gaseous mixtures were prepared by conventional procedures with the use of a greaseless vacuum line. The starting chiral alcohol, ^{18}O-labeled water (^{18}O content > 97%), the thermal radical scavenger O_2, and a powerful base B = $(C_2H_5)_3N$ were introduced into carefully outgassed 130 mL Pyrex bulbs, each equipped with a break-seal tip. The bulbs were filled with CH_3F or CH_3Cl (720 Torr), cooled to liquid-nitrogen temperature, and sealed off. The gaseous mixtures were submitted to irradiation at a constant temperature (25−100 °C) in a ^{60}Co source (dose, 2 × 10^4 Gy; dose rate, 1 × 10^4 Gy h^{-1}, determined with a neopentane dosimeter). Control experiments, carried out at doses ranging from 1 × 10^4 to 1 × 10^5 Gy, showed that the relative yields of products are largely independent of the dose. The radiolytic products were analyzed by GLC, with a Perkin-Elmer 8700 gas chromatograph equipped with a flame ionization detector, on the same columns used to analyze the starting alcohols $\mathbf{1_R^X}$. The products were identified by comparison of their retention volumes with those of authentic standard compounds and their identities confirmed by GLC−MS, using a Hewlett-Packard 5890 A gas chromatograph in line with a HP 5970 B mass spectrometer. Their yields were determined from the areas of the corresponding eluted peaks, using an internal standard (benzyl alcohol) and individual calibration factors to correct for the detector response. Blank experiments were carried out to exclude the occurrence of thermal decomposition and racemization of the starting alcohols as well as of their ethereal products within the temperature range investigated.

The extent of ^{18}O incorporation into the radiolytic products was determined by GLC−MS, setting the mass analyzer in the selected ion mode (SIM). The ion fragments at *m*/*z* = 121 (^{16}O−[M − CH_3]$^+$) and 123 (^{18}O−[M − CH_3]$^+$) were monitored to analyze the $\mathbf{2_S^H}$ and $\mathbf{2_R^H}$ ethers. The corresponding alcohols $\mathbf{1_S^H}$ and $\mathbf{1_R^H}$ were examined by using the fragments at *m*/*z* = 107 (^{16}O−[M − CH_3]$^+$) and *m*/*z*=109 (^{18}O-[M-CH_3]$^+$). The ion fragments at *m*/*z*=211 (^{16}O-[M-CH_3]$^+$) and 213 (^{18}O−[M − CH_3]$^+$) were monitored to analyze the $\mathbf{2_S^F}$ and $\mathbf{2_R^F}$ ethers. The corresponding alcohols $\mathbf{1_S^F}$ and $\mathbf{1_R^F}$ were examined by using the fragments at *m*/*z* = 197 (^{16}O−[M − CH_3]$^+$) and 199 (^{18}O−[M − CH_3]$^+$).

Table 1. Gas-Phase Intracomplex Substitution in Adduct $\mathbf{I^H}$ [a]

reactn temp (°C)	Et_3N (Torr)	reactn time (τ, ×10^8 s)	$[\mathbf{2_R^H}]/[\mathbf{2_S^H}]$[b]	$1-\alpha^{H}$ [c]	α^{H} [c]	k_{front}/k_{back}
25	1.15	2.2	1.296	0.984	0.016	1.31
30	1.25	2.0	1.217	0.980	0.020	1.23
40	1.42	1.9	1.092	0.977	0.023	1.10
60	1.15	2.4	1.000	0.947	0.053	1.00
70	1.10	2.6	0.984	0.925	0.075	0.98
80	1.16	2.6	0.978	0.907	0.093	0.97
100	1.18	2.7	0.985	0.855	0.145	0.98

[a] CH_3F, 720 Torr; O_2, 4 Torr; $\mathbf{1_R^H}$, 0.6−0.8 Torr. Radiation dose, 2 × 10^4 Gy (dose rate, 1 × 10^4 Gy h^{-1}) [b] Each value is the average of several determinations, with an uncertainty level of ca. 5%. [c] α^H derived from the Arrhenius equation for the $\mathbf{II_R^H}$ inversion (Table 3).

Table 2. Gas-Phase Intracomplex Substitution in Adduct $\mathbf{I^F}$ [a]

reactn temp (°C)	Et_3N (Torr)	reactn time (τ, ×10^8 s)	$[\mathbf{2_R^F}]/[\mathbf{2_S^F}]$[b]	$1-\alpha^{F}$ [c]	α^{F} [c]	k_{front}/k_{back}
25	0.53	5.2	7.499	0.992	0.008	7.99
40	0.51	5.7	5.141	0.981	0.019	5.69
60	0.46	6.7	3.410	0.949	0.051	4.11
70	0.39	8.1	2.823	0.911	0.089	3.77
80	0.39	8.5	2.073	0.872	0.128	2.77
100	0.46	7.5	1.461	0.797	0.203	1.92

[a] CH_3F, 720 Torr; O_2, 4 Torr; $\mathbf{1_R^F}$, 0.2−0.4 Torr. Radiation dose, 2 × 10^4 Gy (dose rate, 1 × 10^4 Gy h^{-1}). [b] Each value is the average of several determinations, with an uncertainty level of ca. 5%. [c] α^F derived from the Arrhenius equation for the $\mathbf{II_R^F}$ inversion (Table 4).

Results

Tables 1 and 2 report the $[\mathbf{2_R^X}]/[\mathbf{2_S^X}]$ ratio of the ^{18}O-labeled ethers recovered in the $CH_3F/H_2{}^{18}O/\mathbf{1_R^X}$ gaseous samples.

(12) Speranza, M.; Troiani, A. *J. Org. Chem.* **1998**, *63*, 1020.

(13) A direct proof of the inertness of $(CH_3)_2Cl^+$ ions toward water arises from the observation that the ethereal products, recovered in the $CH_3Cl/H_2{}^{18}O/\mathbf{1_R^X}$ mixtures, contain less than 3% of the ^{18}O label.

(14) Achet, D.; Rocrelle, D.; Murengezi, I.; Delmas, A.; Gaset, A. *Synthesis* **1986**, 643.

Table 3. Gas-Phase Unimolecular Inversion of Oxonium Ion $\mathbf{II_R^H}$ [a]

reactn temp (°C)	Et_3N (Torr)	reactn time (τ, $\times 10^8$ s)	yield factors[b] $1-\alpha^H$	yield factors[b] α^H	k_{inv} ($\times 10^{-6}$ s^{-1})
25	1.22	2.1	0.985	0.015	0.7
60	1.20	2.3	0.947	0.053	2.4
85	1.20	2.5	0.882	0.118	5.4
100	1.20	2.6	0.867	0.133	5.9
120	1.20	2.8	0.803	0.197	8.9
140	1.20	2.9	0.707	0.293	15.2
140	1.20	2.9	0.719	0.281	14.2
160	1.20	3.1	0.643	0.357	20.2

[a] CH_3Cl, 720 Torr; O_2, 4 Torr; $\mathbf{1_R^H}$, 0.5−0.6 Torr. Radiation dose, 2×10^4 Gy (dose rate, 1×104 Gy h^{-1}). [b] $\alpha^H = [\mathbf{2_S^H}]/([\mathbf{2_R^H}] + [\mathbf{2_S^H}])$, $(1 - \alpha^H) = [\mathbf{2_R^H}]/([\mathbf{2_R^H}]+[\mathbf{2_S^H}])$. Each value is the average of several determinations, with an uncertainty level of ca. 5%.

Table 4. Gas-Phase Unimolecular Inversion of Oxonium Ion $\mathbf{II_R^F}$ [a]

reactn temp (°C)	Et_3N (Torr)	reactn time (τ, $\times 10^8$ s)	yield factors[b] $1-\alpha^H$	yield factors[b] α^H	k_{inv} ($\times 10^{-6}$ s^{-1})
25	0.46	5.2	0.996	0.004	0.08
60	0.49	6.2	0.974	0.026	0.43
85	0.51	6.5	0.931	0.069	1.14
120	0.54	6.8	0.772	0.228	4.48
160	0.42	9.6	0.547	0.453	12.30

[a] CH_3Cl, 720 Torr; O_2, 4 Torr; $\mathbf{1_R^F}$, 0.6−1.0 Torr. Radiation dose, 2×10^4 Gy (dose rate, 1×104 Gy h^{-1}). [b] $\alpha^F = [\mathbf{2_S^F}]/([\mathbf{2_R^F}] + [\mathbf{2_S^F}])$, $(1 - \alpha^F) = [\mathbf{2_R^F}]/([\mathbf{2_R^F}] + [\mathbf{2_S^F}])$. Each value is the average of several determinations, with an uncertainty level of ca. 5%.

Tables 3 and 4 show the yield factors of unlabeled[13] $\mathbf{2_R^X}$ (denoted as $1-\alpha^X$) and $\mathbf{2_S^X}$ (denoted as α^X) from the $CH_3Cl/H_2{}^{18}O/\mathbf{1_R^X}$ gaseous mixtures. The numbers in the tables represent average values obtained from several separate irradiations carried out under the same experimental conditions, and whose reproducibility is expressed by the uncertainty level quoted. The ionic origin of ethers $\mathbf{2_R^X}$ and $\mathbf{2_S^X}$ is demonstrated by the sharp decrease (over 80%) of their abundance as the $(C_2H_5)_3N$ concentration is quintupled.

As pointed out above, the ^{18}O-labeled ethers recovered in the $CH_3F/H_2{}^{18}O/\mathbf{1_R^X}$ gaseous samples (Tables 1 and 2) derive from the intracomplex "solvolysis" of $\mathbf{I^X}$. By contrast, the unlabeled ethers recovered in the $CH_3Cl/H_2{}^{18}O/\mathbf{1_R^X}$ gaseous mixtures (Tables 3 and 4) derive from direct attack of $(CH_3)_2Cl^+$ on $\mathbf{1_R^X}$, and their distribution reflects the extent of the $\mathbf{II_R^X}$ racemization. In both cases, the relative distribution of the ethereal products, e.g., $\mathbf{2_R^H}$ and $\mathbf{2_S^H}$, can be taken as representative of that of the relevant ionic precursors, e.g., $\mathbf{II_R^H}$ and $\mathbf{II_S^H}$, with the reasonable assumption that the neutralization efficiency of the latter by the strong base $B = (C_2H_5)_3N$ (proton affinity (PA) = 234.7 kcal mol^{-1})[15] is close to unity.

According to Scheme 1, the rate constant ratio k_{front}/k_{back} for the frontside vs the backside intracomplex "solvolysis" of $\mathbf{I^X}$ can be expressed by the $[\mathbf{2_R^X}]/[\mathbf{2_S^X}]$ ratio, once corrected by the $\mathbf{II_R^X} \rightleftarrows \mathbf{II_S^X}$ interconversion during their lifetime τ. In the framework of the above assumption, τ is expressed by the collision frequency between $\mathbf{II_R^X}$ and $\mathbf{II_S^X}$ and B ($\tau = (k_b[B])^{-1}$) at each temperature.[16]

(15) Lias, S. G.; Hunter, E. P. L. *J. Phys. Chem. Ref. Data* **1998**, *27*, 413.

(16) The collision constant k_b between the ions of Scheme 1 and $(C_2H_5)_3N$ is calculated as in the following: Su, T.; Chesnavitch, W. J. *J. Chem. Phys.* **1982**, *76*, 5183.

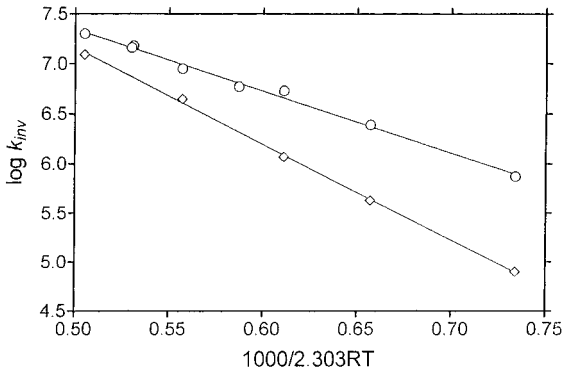

Figure 1. Arrhenius plots for the $\mathbf{II_R^H} \rightleftarrows \mathbf{II_S^H}$ (○) and $\mathbf{II_R^F} \rightleftarrows \mathbf{II_S^F}$ (◇) rearrangements.

The rate constants of $\mathbf{II_R^X}$ inversion can be calculated from the relevant α^X terms of Tables 3 and 4 according to the following equation:[17]

$$1 - 2\alpha^X = e^{-2k_{inv}t} \qquad \text{(eq IV of Appendix)}$$

The Arrhenius plots of k_{inv} over the 25−160 °C temperature range are reported in Figure 1. The linear curves obey the Arrhenius equations reported in entries i ($\mathbf{II_R^H}$) and ii ($\mathbf{II_R^F}$) of Table 5. The same table gives the relevant activation parameters as well, as calculated from the transition-state theory equation.

Taking into account that, during their lifetime τ, the α^X fraction of the intermediates $\mathbf{II_R^X}$ undergoes inversion, the $[\mathbf{2_R^X}]/[\mathbf{2_S^X}]$ ratios of Tables 1 and 2 can be expressed by the following equation:

$$\frac{[\mathbf{2_R^X}]}{[\mathbf{2_S^X}]} = \beta = \frac{k_{front}(1-\alpha^X) + k_{back}\alpha^X}{k_{back}(1-\alpha^X) + k_{front}\alpha^X} \qquad \text{(eq VI of Appendix)}$$

which gives by rearrangement,

$$\frac{k_{front}}{k_{back}} = \frac{\beta(1-\alpha^X) - \alpha^X}{(1-\alpha^X) - \beta\alpha^X} \qquad \text{(eq VII of Appendix)}$$

The relevant k_{front}/k_{back} ratios are reported in Tables 1 and 2, and their temperature dependence is illustrated in Figure 2.

A linear $\log(k_{front}/k_{back})$ vs T^{-1} curve is observed for the intracomplex "solvolysis" of $\mathbf{I^F}$ over the entire 25−100 °C temperature range which obeys the Arrhenius equation in entry iv of Table 5. On the other hand, the $\log(k_{front}/k_{back})$ for the intracomplex "solvolysis" of $\mathbf{I^H}$ is linearly correlated with T^{-1} only below 50 °C (Arrhenius equation in entry iii of Table 5), while it reaches the limiting value of zero at temperatures above 50 °C. This means that above this temperature limit, intracomplex "solvolysis" of $\mathbf{I^H}$ yields the $\mathbf{II_R^H}-\mathbf{II_S^H}$ racemate, whereas at $T < 50$ °C it displays a small but appreciable stereoselectivity. In both $\mathbf{I^F}$ and $\mathbf{I^H}$ (at $T < 50$ °C), frontside substitution predominates over backside displacement. The differential activation parameter relative to the equations in entries iii and iv of Table 5 are given in the same table under the relevant $\Delta\Delta H^{\ddagger}$ and $\Delta\Delta S^{\ddagger}$ headings. The difference between the $\Delta\Delta H^{\ddagger}$ and $\Delta\Delta S^{\ddagger}$ values for $\mathbf{I^F}$ versus $\mathbf{I^H}$ are reported under the $\Delta(\Delta\Delta H^{\ddagger})$and $\Delta(\Delta\Delta S^{\ddagger})$ headings of Table 5, respectively.

Discussion

The Gas-Phase Intracomplex "Solvolysis". A recent theoretical and experimental study demonstrates that the rate of the

(17) Filippi, A.; Gasparrini, F.; Speranza, M. *J. Am. Chem. Soc.* **2001**, *123*, 2251.

Table 5. Arrhenius Parameters for the Gas-Phase Inversion of $\mathbf{II_R^X}$ and the Gas-Phase "Solvolysis"of $\mathbf{I^X}$

entry	process	Arrhenius equation ($y = 1000/2.303RT$)	correl coeff (r^2)	$\Delta H^{\ddagger}$(kcal mol^{-1})	$\Delta S^{\ddagger}$(cal mol^{-1} K^{-1})
i	$\mathbf{II_R^H \rightleftarrows II_S^H}$	$\log k_{inv} = (10.4 \pm 0.1) - (6.2 \pm 0.2)y$	0.994	5.4 ± 0.3	-13.3 ± 1.0
ii	$\mathbf{II_R^F \rightleftarrows II_S^F}$	$\log k_{inv} = (12.0 \pm 0.1) - (9.7 \pm 0.2)y$	0.999	8.9 ± 0.2	-5.4 ± 0.5

entry	process	Arrhenius equation ($y = 1000/2.303RT$)	correl coeff (r^2)	$\Delta\Delta H^{\ddagger}$ [a] (kcal mol^{-1})	$\Delta(\Delta\Delta H^{\ddagger})$ [b] (kcal mol^{-1})	$\Delta\Delta S^{\ddagger}$ [c] (cal mol^{-1} K^{-1})	$\Delta(\Delta\Delta S^{\ddagger})$ [d] (cal mol^{-1} K^{-1})
iii	$\mathbf{II_R^H \leftarrow I^H \rightarrow II_S^H}$	$\log(k_{front}/k_{back}) = (-1.5 \pm 0.1) + (2.2 \pm 0.1)y$	1.000	2.2 ± 0.1	1.9 ± 0.3	6.7 ± 0.1	2.8 ± 0.5
iv	$\mathbf{II_R^F \leftarrow I^F \rightarrow II_S^F}$	$\log(k_{front}/k_{back}) = (-2.1 \pm 0.2) + (4.1 \pm 0.3)y$	0.981	4.1 ± 0.3		9.5 ± 0.5	

[a] $\Delta\Delta H^{\ddagger} = \Delta H^{\ddagger}_{back} - \Delta H^{\ddagger}_{front}$. [b] $\Delta(\Delta\Delta H^{\ddagger}) = \Delta\Delta H^{\ddagger}(\mathbf{I^F}) - \Delta\Delta H^{\ddagger}(\mathbf{I^H})$. [c] $\Delta\Delta S^{\ddagger} = \Delta S^{\ddagger}_{back} - \Delta S^{\ddagger}_{front}$. [d] $\Delta(\Delta\Delta S^{\ddagger}) = \Delta\Delta S^{\ddagger}(\mathbf{I^F}) - \Delta\Delta S^{\ddagger}(\mathbf{I^H})$.

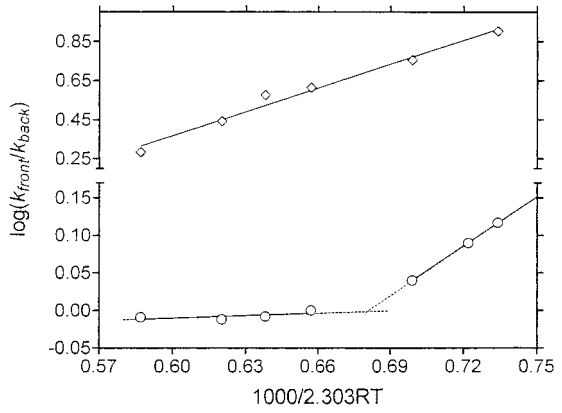

Figure 2. Temperature dependence of the k_{front}/k_{back} ratios for the intracomplex "solvolyses" of $\mathbf{I^H}$ (○) and $\mathbf{I^F}$ (◇).

Scheme 3

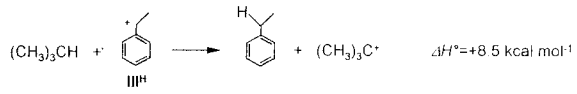

quasi-resonant $H_2{}^{18}O$-to-H_2O substitution on protonated alkanols ROH_2^+ in the isolated state[18] decreases in the order R = $(CH_3)_3C$ > $(CH_3)_2CH$ > CH_3 > CH_3CH_2. This trend is accounted for by the nature of the interactions between the R moiety and the poorly nucleophilic water molecules in the relevant transition structure (TS). The carbocationic character of R increases from CH_3 to $(CH_3)_3C$ owing to the stabilizing effects of the methyl substituent groups. Hence, the covalent character of the $H_2O\cdots C\cdots OH_2$ interactions decreases in the same order. Frontside substitution becomes competitive with the classical backside displacement with increasing R^+ stabilization. In the case of highly stabilized R^+, it is thought that the limiting frontside and backside pathways may merge into the S_N1 mechanism. Another relevant aspect is that the activation barrier associated with the motion of the H_2O nucleophile around ROH_2^+ is found to decrease with increasing stability of the R^+ carbocation.[19]

In accordance with common practice, the enthalpy change of the isodesmic reaction given in Scheme 3 provides a measure of the stabilization energy of the α-methyl benzyl cation ($\mathbf{III^H}$) relative to that of the *tert*-butyl cation.[15] The high stability of ion $\mathbf{III^H}$ suggests that the exothermic intracomplex displacement in $\mathbf{I^H}$ proceeds through TSs characterized by noncovalent interactions between $\mathbf{III^H}$ and the nucleophile/leaving group pair (an S_N1 process). The formation of the $\mathbf{II_R^H - II_S^H}$ racemate from

Chart 1

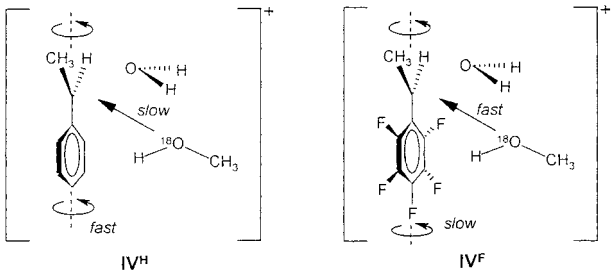

$\mathbf{I^H}$ at $T > 50$ °C is entirely consistent with this view. In this frame, the slight predominance of retained $\mathbf{II_R^H}$ over the inverted $\mathbf{II_S^H}$, observed at $T < 50$ °C, can be accounted for by a free rotation of the benzylic moiety of complex $\mathbf{IV^H}$ (Chart 1), slower than its bonding to $CH_3{}^{18}OH$. In fact, the procedure adopted to generate $\mathbf{I^H}$ in the gas phase requires that the $CH_3{}^{18}OH$ moiety reside initially in the same region of space containing the leaving group (complex $\mathbf{IV^H}$ in Chart 1). In the absence of any intracomplex rotation of the benzylic moiety of $\mathbf{IV^H}$, $CH_3{}^{18}OH$ is spatially situated to attack from the frontside. At higher temperatures, this positional advantage is annulled, and the $\mathbf{II_R^H - II_S^H}$ racemate is formed. The phenomenological $\Delta\Delta H^{\ddagger} = (\Delta H^{\ddagger}_{back} - \Delta H^{\ddagger}_{front}) = 2.2 \pm 0.1$ kcal mol^{-1} and $\Delta\Delta S^{\ddagger} = (\Delta S^{\ddagger}_{back} - \Delta S^{\ddagger}_{front}) = 6.7 \pm 0.1$ cal mol^{-1} K^{-1} values, measured for the $\mathbf{I^H}$ intracomplex "solvolysis" (entry iii of Table 5), reflect the difference between the activation parameters for rotation of the benzylic moiety in the electrostatic complex $\mathbf{IV^H}$ versus those for its addition to $CH_3{}^{18}OH$.

Selective reactions controlled by the initial spatial correlation of the reactants are by no means infrequent in organic chemistry.[20] In them, named by Hoveyda and Evans as "substrate-directable reactions",[21] the substrate is equipped with a remote functionality suitable to coordinate the reactant and deliver it selectively to a given reaction site. The preferred retention of configuration in the intracomplex "solvolysis" of $\mathbf{I^H}$ is a rare example of substrate-directable gas-phase reactions,[22] in which the reagent (i.e., $CH_3{}^{18}OH$) is not preformed but rather generated in the complex by $CH_3{}^{18}OH_2^+$ proton transfer to $\mathbf{1_R^H}$. Besides, $CH_3{}^{18}OH$ is oriented not by coordination with a remote functionality, but with the leaving group itself. The term "troposelective" [23] is proposed to classify this particular version of substrate-directable reactions. Thus, "troposelectivity" stands for the selectivity of a reagent toward the chiral or prochiral face of a substrate on which it has been generated.

(18) Uggerud, E.; Bache-Andreassen, L. *Chem. Eur. J.* **1999**, *5*, 1917.

(19) This is true in going from R = CH_3 to R = $(CH_3)_2CH$, where the moving H_2O interacts primarily with hydrogens directly bound to the formally charged carbon. When R = $(CH_3)_3C$, no such hydrogens are available, and the activation barrier associated with the motion of the H_2O nucleophile around ROH_2^+ increases slightly.

(20) Breit, B. *Chem. Eur. J.* **2000**, *6*, 1519.

(21) Hoveyda, A. H.; Evans, D. A.; Fu, G. C. *Chem. Rev.* **1993**, *93*, 1307.

(22) Other examples of gas-phase positionally oriented reactions are reported in ref 12 and in the following: Cecchi, P.; Pizzabiocca, A.; Renzi, G.; Chini, M.; Crotti, P.; Macchia, F.; Speranza, M. *Tetrahedron* **1989**, *45*, 4227.

(23) Troposelectivity is a term coined from the combination of the Greek word "τροπός" (turning) and the Latin word "selectu(m)" from the verb "seligere" (to select).

The intracomplex "solvolysis" of $\mathbf{I^F}$ can be considered highly troposelective since it involves predominant retention of configuration (88% at 25 °C). Inductive and resonance effects of the ring fluorine substituents reduce appreciably the stabilization energy of α-methyl pentafluorobenzyl cation ($\mathbf{III^F}$) relative to that of $\mathbf{III^H}$.[24] This implies that the interactions between the nucleophile/leaving group and benzylic moiety in complex $\mathbf{IV^F}$ (Chart 1) should be stronger than those operating in adduct $\mathbf{IV^H}$. In principle, this condition could lead to a change of mechanism from S_N1 to S_N2. However, according to analogous gas-phase S_N2 reactions[25,26] and theoretical predictions,[18] intracomplex S_N2 displacements generally involve substantial activation barriers and proceed via predominant inversion of configuration, in contrast to the present observations. More convincing is the hypothesis that "solvolysis" of $\mathbf{I^F}$ follows the same unimolecular mechanism as $\mathbf{I^H}$, with the only difference being that the stronger interactions in $\mathbf{IV^F}$ hinder free rotation of benzylic moiety with respect to its recombination with $CH_3{}^{18}OH$. This view is supported by the differential activation parameters for the $\mathbf{I^X}$ intracomplex "solvolysis" reported under the $\Delta(\Delta\Delta H^{\ddagger})$and $\Delta(\Delta\Delta S^{\ddagger})$ headings of Table 5. Assuming similar activation enthalpy and entropy for recombination of the benzylic moiety and $CH_3{}^{18}OH$ in the relevant $\mathbf{IV^X}$, the $\Delta(\Delta\Delta H^{\ddagger}) = (\Delta\Delta H^{\ddagger}(\mathbf{I^F}) - \Delta\Delta H^{\ddagger}(\mathbf{I^H})) = 1.9 \pm 0.3$ kcal mol^{-1} and $\Delta(\Delta\Delta S^{\ddagger}) = (\Delta\Delta S^{\ddagger}(\mathbf{I^F}) - \Delta\Delta S^{\ddagger}(\mathbf{I^H})) = 2.8 \pm 0.5$ cal mol^{-1} K^{-1} are consistent with a rearrangement of the tighter complex $\mathbf{IV^F}$ involving higher activation enthalpies and entropies than that of the looser complex $\mathbf{IV^H}$.

Comparison with Related Gas-Phase and Solution Data. The idea of troposelective intracomplex reactions in the gas phase has its origin in a comprehensive investigation of acid-induced displacement reactions by Beauchamp and co-workers.[27] These authors were originally interested in the mechanism of nucleophilic displacements in proton-bound complexes between alkyl halides and several nucleophiles. No indication was given as to the stereochemistry of the process. However, according to the geometry proposed for the proton-bound complexes (analogous to those depicted in Chart 1), a frontside substitution should predominate in Beauchamp's adducts that, if involving chiral alkyl halides, should cause the retention of configuration of the reaction center. The hypothesis of frontside attack in gas-phase nucleophilic substitutions has been checked by mass spectrometric,[28−30] theoretical,[31] and radiolytic[26,32] methods. The mass spectrometric approach led to contrasting conclusions. In their ICR study of the reaction between $CH_3{}^{16}OH$ and $CH_3{}^{18}OH_2{}^+$, Kleingeld and Nibbering concluded that nucleophilic attack takes place predominantly from the backside.[28] Their view is at odds with the experimental results of Bowers et al., pointing to the reaction as proceeding essentially via the proton-bound adduct and, therefore, involving frontside attack.[29] The picture is made even fuzzier by ab initio theoretical calculations which indicate that the proton-bound adduct, preferentially generated in the $CH_3OH/CH_3OH_2{}^+$ encounter, may undergo rearrangement prior to backside S_N2 substitution.[31] Detailed information on the stereochemistry of a number of acid-induced gas-phase nucleophilic substitutions was obtained by applying the radiolytic technique which, contrary to mass spectrometry, is based on the isolation and structural identification of the neutral reaction products.[32] In these studies, the reaction was carried out by generating the protonated substrate *in the presence of appreciable concentrations of the nucleophile*. Under such conditions, the reaction invariably takes place with predominant inversion of configuration. It is thought that the collision between the protonated substrate and the nucleophile yields predominantly a proton-bound complex that is structurally similar to $\mathbf{I^X}$. If sufficiently long-lived,[33] this complex may undergo attack by *another* molecule of nucleophile from its unshielded backside.[32] The present gas-phase results substantiate this hypothesis. Indeed, if the proton-bound adduct between the nucleophile and the substrate (e.g., $\mathbf{I^F}$) is formed *in the absence of the neutral nucleophile* (i.e., $CH_3{}^{18}OH$), the intracomplex displacement reaction takes place with predominant retention of configuration.

The above gas-phase picture may represent a guideline for understanding the mechanism and the stereochemistry of solvolytic reactions in the solvent cage. The results of gas-phase $\mathbf{1_R^H}$ "solvolysis" demonstrate the existence of a pure S_N1 mechanism. Fast rotation of the ion $\mathbf{III^H}$ in the complex $\mathbf{IV^H}$ ($T > 50$ °C) explains the formation of the product racemate. If rotation is hampered by significant ion−nucleophile interactions (as in $\mathbf{I^F}$ and $\mathbf{I^H}$ at $T < 50°$), predominant retention of configuration is observed. This may explain why some solvolytic reactions lead to a slight excess of the retained product in the liquid phase.[22,34−38] However, the presence of the solvent cage may alter this picture and favor inversion of configuration, even if a pure S_N1 solvolysis is taking place. This may happen when reorientation of the ion in the cage is slow and if the presence of the leaving group somewhat hampers the approach of the nucleophile from the frontside. However, inversion of configuration predominates even when the relative motionlessness of the ion in the solvent cage is due to a partial covalency of its interactions with the leaving group and the nucleophilic solvent (a S_N2 process). It is concluded that the solvolytic reactions are mostly governed by the lifetime and the dynamics of the species involved and, if occurring in solution, by the nature of the solvent cage. Their rigid subdivision into the S_N1 and S_N2 mechanistic categories appears inadequate, and the use of their stereochemistry as a mechanistic probe can be highly misleading.

Acknowledgment. This work was supported by the Ministero della Università e della Ricerca Scientifica e Tecnologica

(24) Marcuzzi, F.; Modena, G.; Paradisi, C.; Giancaspro, C.; Speranza, M. *J. Org. Chem.* **1985**, *50*, 4937.

(25) (a) Filippi, A.; Speranza, M. *Int. J. Mass Spectrom. Ion Processes* **1999**, *185/186/187*, 425. (b) Troiani, A.; Filippi, A.; Speranza, M. *Chem. Eur. J.* **1997**, *3*, 2063.

(26) Hall, D. G.; Gupta, C.; Morton, T. H. *J. Am. Chem. Soc.* **1981**, *103*, 2416.

(27) Beauchamp, J. L. In *Interactions between Ions and Molecules*; Ausloos, P., Ed; Plenum Press: New York, 1975, and references therein.

(28) Kleingeld, J. C.: Nibbering, N. M. M. *Org. Mass Spectrom.* **1982**, *17*, 136. The conclusions of this work are based on the observation of a predominant signal, corresponding to $(CH_3)_2{}^{16}OH^+$, and a minor one, corresponding to $(CH_3)_2{}^{16}OH^+$. However, the same $(CH_3)_2{}^{16}OH^+$ product can be obtained also by the frontside displacement.

(29) Bass, L. M.; Cates, R. D.; Jarrold, M. F.; Kirchner, N. J.; Bowers, M. T. *J. Am. Chem. Soc.* **1983**, *105*, 7024.

(30) Bierbaum, V. M.; Dang, T. T. *Int. J. Mass Spectrom. Ion Processes* **1992**, *117*, 65 and references therein.

(31) (a) Bouchoux, G.; Choret, N. *Rapid Commun. Mass Spectrom.* **1997**, *11*, 1799. (b) Sheldon, J. C.; Currie, G. J.; Bowie, J. H. *J. Chem. Soc., Perkin Trans. 2* **1986**, 941. (c) Fridgen, T. D.; Keller, J. D.; McMahon, T. B. *J. Phys. Chem.* **2001**, *105*, 3816.

(32) Speranza, M.; Angelini, G. *J. Am. Chem. Soc.* **1980**, *102*, 3115.

(33) Experimental evidence in favor of this conclusion is reported in ref 22.

(34) Merritt, M. V.; Bronson, G. E. *J. Am. Chem. Soc.* **1978**, *100*, 1891.

(35) Merritt, M. V.; Bronson, G. E., Baczynskyj, L.; Boal, J. R. *J. Am. Chem. Soc.* **1978**, *100*, 1891.

(36) Merritt, M. V.; Bell, S. J.; Cheon, H. J.; Darlington, J. A.; Dugger, T. L.; Elliott, N. B.; Fairbrother, G. L.; Melendez, C. S.; Smith, E. V.; Schwartz, P. L. *J. Am. Chem. Soc.* **1990**, *112*, 3560.

(37) Merritt, M. V.; Anderson, D. B.; Basu, K. A.; Chang, I. W.; Cheon, H. J.; Mukundan, N. E.; Flannery, C. A.; Kim, A. Y.; Vaishampayan, A.; Yens, D. A. *J. Am. Chem. Soc.* **1994**, *116*, 5551.

(38) Allen, A. D.; Kanagasabapathy, V. M.; Tidwell, T. T. *J. Am. Chem. Soc.* **1985**, *107*, 4513.

(MURST) and the Consiglio Nazionale delle Ricerche (CNR). We thank F. Gasparrini for his continuous encouragement and invaluable assistance in the purification of the starting chiral alcohols.

Appendix

In the $\mathbf{II_R}^X \rightleftarrows \mathbf{II_S}^X$ inversion (Scheme 1), if initially only $\mathbf{II_R}^X$ is present with a yield factor $[\mathbf{II_R}^X] = 1$ and its fraction α^X has reacted at time t, then the differential equation,

$$\frac{d[\mathbf{II_S}^X]}{dt} = k_{inv}[\mathbf{II_R}^X] - k_{inv}[\mathbf{II_S}^X] \quad \text{(I)}$$

may be rewritten with $[\mathbf{II_R}^X] = 1 - \alpha^X$ and $[\mathbf{II_S}^X] = \alpha^X$:

$$\frac{d\alpha^X}{dt} = k_{inv}(1 - 2\alpha^X) \quad \text{(II)}$$

By integrating eq II and considering that $\alpha^X = 0$ at $t = 0$ and $\alpha^X = 0.5$ at $t = \infty$,

$$\ln\left\{\frac{1}{(1 - 2\alpha^X)}\right\} = 2k_{inv}t \quad \text{(III)}$$

Thence,

$$1 - 2\alpha^X = e^{-2k_{inv}t} \quad \text{(IV)}$$

According to Scheme 1, the measured $[\mathbf{2_R}^X]$ vs $[\mathbf{2_S}^X]$ yield ratios of Tables 1 and 2 may be expressed as

$$\frac{[\mathbf{2_R}^X]}{[\mathbf{2_S}^X]} = \frac{k_{front}[\mathbf{I}^X] + k_{inv}[\mathbf{II_S}^X] - k_{inv}[\mathbf{II_R}^X]}{k_{back}[\mathbf{I}^X] + k_{inv}[\mathbf{II_R}^X] - k_{inv}[\mathbf{II_S}^X]} \quad \text{(V)}$$

which may be reduced:

$$\frac{[\mathbf{2_R}^X]}{[\mathbf{2_S}^X]} = \beta = \frac{k_{front}(1 - \alpha^X) + k_{back}\alpha^X}{k_{back}(1 - \alpha^X) + k_{front}\alpha^X} \quad \text{(VI)}$$

Thence,

$$\frac{k_{front}}{k_{back}} = \frac{\beta(1 - \alpha^X) - \alpha^X}{(1 - \alpha^X) - \beta\alpha^X} \quad \text{(VII)}$$

JA004265P